Journal of Natural Fibers

ISSN: (Print) (Online) Journal homepage: informahealthcare.com/journals/wjnf20

Biosynthesis of Silver Nanoparticles Enhanced Antibacterial Silk Face Covering

Phannaphat Phromphen, Udomlak Sukatta, Prapassorn Rugthaworn, Jirachaya Boonyarit, Phitalai Phoophat, Nattadon Rungruangkitkrai, Pawarin Tuntariyanond, Nawarat Chartvivatpornchai, Thanyachol Apipatpapha & Rungsima Chollakup

To cite this article: Phannaphat Phromphen, Udomlak Sukatta, Prapassorn Rugthaworn, Jirachaya Boonyarit, Phitalai Phoophat, Nattadon Rungruangkitkrai, Pawarin Tuntariyanond, Nawarat Chartvivatpornchai, Thanyachol Apipatpapha & Rungsima Chollakup (2023) Biosynthesis of Silver Nanoparticles Enhanced Antibacterial Silk Face Covering, Journal of Natural Fibers, 20:2, 2212926, DOI: 10.1080/15440478.2023.2212926

To link to this article: https://doi.org/10.1080/15440478.2023.2212926

Published online: 23 May 2023.

JOURNAL OF NATURAL FIBERS
2023, VOL. 20, NO. 2, 2212926
https://doi.org/10.1080/15440478.2023.2212926

Biosynthesis of Silver Nanoparticles Enhanced Antibacterial Silk Face Covering

Phannaphat Phromphen[a], Udomlak Sukatta[b], Prapassorn Rugthaworn[b], Jirachaya Boonyarit[b], Phitalai Phoophat[a], Nattadon Rungruangkitkrai[a], Pawarin Tuntariyanond[a], Nawarat Chartvivatpornchai[a], Thanyachol Apipatpapha[b], and Rungsima Chollakup[b]

[a]Department of Textile Science, Faculty of Agro-Industry, Kasetsart University, Bangkok, Thailand; [b]Kasetsart Agricultural and Agro-Industrial Product Improvement Institute, Kasetsart University, Bangkok, Thailand

ABSTRACT

Biosynthesis of silver nanoparticles (AgNPs) using plant extracts as reducing agents has recently attracted interest as an environmentally friendly and cost-effective approach. In this study, biosynthesized silver nanoparticles were coated on cotton fabric as an antimicrobial outer middle layer in a silk face mask. The AgNPs were synthesized and characterized by scanning electron microscopy (SEM) and energy-dispersive X-ray spectroscopy (EDX). A solution of 100 ppm AgNPs was coated on cotton fabric by the exhaustion process and quantified according to the procedures of AATCC 100–1999. Top performance characteristics of the barrier face covering were determined according to ASTM F3502–2021. The AgNPs were spherical with particle size ranging 35–88 nm. SEM images of AgNP-coated cotton fabrics showed good particle dispersion that decreased after washing, with 99% reduction in viable *E. coli* and *S. aureus* after 30 washing cycles. The developed silk face covering also offered sufficient sub-micron particle filtration efficiency and airflow resistance as level II performance under ASTM classification.

摘要

最近, 使用植物提取物作为还原剂生物合成银纳米颗粒(AgNP)作为一种环境友好且具有成本效益的方法引起了人们的兴趣. 在这项研究中, 将生物合成的银纳米颗粒涂覆在棉布上, 作为丝绸口罩中的抗菌外中间层. 合成了AgNPs, 并通过扫描电子显微镜(SEM)和能量色散X射线光谱(EDX)对其进行了表征. 将100ppm AgNP的溶液通过穷竭法涂布在棉布上, 并根据AATCC 100-1999的程序进行定量. 根据ASTM F3502-2021测定阻挡面覆盖物的顶部性能特征. AgNPs是球形的, 颗粒尺寸范围为35-88 nm. AgNP涂层棉织物的SEM图像显示出良好的颗粒分散性, 洗涤后颗粒分散性降低, 30次洗涤循环后, 活大肠杆菌和金黄色葡萄球菌减少99%. 所开发的丝绸面部覆盖物还提供了足够的亚微米颗粒过滤效率和气流阻力, 作为ASTM分类的II级性能.

KEYWORDS

Mangosteen; Eri silk; environmentally friendly; filtration efficiency; airflow resistance; mask

关键词

山竹; 伊利丝绸; 环境友好; 过滤效率; 气流阻力; 面具

Introduction

During the COVID-19 pandemic, N95, FFP2, and FFP3 respirators and medical masks were highly recommended for healthcare workers, with non-medical masks suggested for the general public (World Health Organization 2020). The filtration and particle capture mechanisms of N95 respirators and surgical masks filter out smaller particulate matter, bacteria, and

CONTACT Rungsima Chollakup aaprmc@ku.ac.th Kasetsart Agricultural and Agro-Industrial Product Improvement Institute, Kasetsart University, Bangkok 10900, Thailand

viruses (Adanur and Jayswal 2020). Surgical masks and N95 respirators are usually made from thermoplastic nonwoven fabrics, with the designs intended as a protective barrier providing fluid resistance. Non-medical or homemade masks, such as scarves or bandanas do not filter aerosol sizes between 30 and 600 nm but can capture large respiratory droplets, which are a significant mode of transmission of SRS-CoV-2 (Hao et al. 2020). These masks for public use are normally made from easily and inexpensive materials, such as cotton, silk, linen, and wool. Multi-layered structures of woven fabric can exceed the efficiency of materials used in some medical face masks (Zhao et al. 2020). These fabric masks have low filtration efficiency and retain moisture, favoring bacterial or viral organisms that might cause risk of infection (MacIntyre et al. 2015). Pore size of fabric masks expands after rubbing, with damage to the sample caused by abrasion. Therefore, fabric masks are not recommended for healthcare workers (Davies et al. 2013).

The new standard "*ASTM F3502 standard specification for barrier face coverings*" was established in response to the global COVID-19 pandemic to describe a product that was neither a medical mask nor an inhalation protection respirator. Principal performance criteria for face covering only emphasized sub-micron particle filtration efficiency and airflow resistance (American Society for Testing and Materials 2021). Particulate filtration efficiency was quantified as the ability of the face covering to remove aerosol particles passing through the material, while airflow resistance properties indicated mask comfort and breathability. Airflow resistance could be measured by differential pressure. The higher the differential pressure, the harder it was to breathe when wearing the mask (Forouzandeh, O'Dowd, and Pillai 2021). Lima et al. (2022) also suggested that an airflow resistance value of the respirator above 8 mm H_2O was considered unbreathable. Compared with medical surgical masks and N95, FFP2, or FFP3 respirators, this new standard of face coverings also reduced the risk of virus infection and effectively prevented pathogens from spreading in the environment. Face coverings that meet the ASTM F3502 requirement could be used by the general public. Functional properties such as antimicrobial (Kharaghani et al. 2018; Li et al. 2006) and water repellence (Ray et al. 2020) could also be added to the face covering.

Silk is a decent material for fabric masks; it had a high hydrophobic barrier to droplets and was breathable and reusable after cleaning (Parlin et al. 2020). Four layers of silk fabric protected against particulate penetration ranging from 10 nm to 6 μm (Konda et al. 2020), while the silk filament showed high rubbing resistance, low chance of pilling, excellent antimicrobial property, and good air permeability (Kaur et al. 2014; Phoophat et al. 2020). Eri silk, a protein fiber derived from cocoons made by wild silk moths, also showed the unique characteristics of lightness, soft-smooth feel, thermal property, and high tensile strength (Chollakup and Smitthipong 2012; Rungruangkitkrai et al. 2020).

An antimicrobial textile inhibited the growth of bacterial infections through the material (Abou Elmaaty et al. 2022). However, the protective layer of the face mask was not able to filler microorganisms, which may cause a health risk to the user (Hiragond et al. 2018). Silver nanoparticles (AgNPs) had been used to produce antimicrobial textiles because of their antibacterial, antifungal, anticancer, anti-inflammatory and UV protection properties (Emam, El-Rafie, and Rehan 2021; Syafiuddin 2019). Biosynthesis of AgNPs was suggested as an alternative method to enhance the antibacterial properties of the face covering and replace chemical and physical processes. This method was more environmentally friendly and cost-effective with reduced use of chemicals (Yaqoob, Umar, and Ibrahim 2020). Previous research reported the utilization of basil (Brahmachari et al. 2014), banana leaves (Ibrahim 2015), banana peel (Bankar et al. 2010) and sweet flag root (Nakkala et al. 2015) to biosynthesize AgNPs that can inhibit microorganisms at lower concentrations than other heavy metals. Moreover, some natural polymers such as chitosan (Hasan et al. 2022; Mohammed, Hassan, and Hassan 2023), pectin (Zhao et al. 2022), xanthan gum (Emam and Zahran 2015), acacia gum (Emam et al. 2015), gum ghatti and gum olibanum (Kora and Sashidhar 2015) were used as the capping and/or reduction of AgNPs in the green synthesis method. In addition, small amounts of AgNPs do not harm eukaryotic cells while destroying bacterial cells in the human body.

This study synthesized AgNPs using green technology. The AgNPs were coated on cotton fabric as an antibacterial layer in the silk face covering. The antimicrobial activities of AgNPs and AgNPs coated on cotton fabric were analyzed by an antibacterial assay. The performance of the face covering for submicron particle filtration efficiency and airflow resistance was also evaluated according to the ASTM standard requirement.

Experimental

Materials

Mangosteen (*Garcinia mangostana* Linn.) peels were purchased from a local grocery store in Bangkok, Thailand. Silk filament fabric 91.62 g/m^2 and Eri silk fabric 74.29 g/m^2 to make the face covering prototype were obtained from Natural Niche Co., Ltd. Silver nitrate ($AgNO_3$) was purchased from Sigma Aldrich. A water-repellent agent, namely perfluorooctanoic acid-free fluorocarbon (PFOA-free fluorocarbon) was purchased from Star Tech Chemical Co., Ltd. (Bangkok, Thailand).

Preparation of peel extract

To make the aqueous mangosteen peel extract, the fruit peels were first washed with deionized water, then cut into small pieces and dried in a hot air oven at 60°C until moisture content was less than 8%. The dry mangosteen peels were then ground to a coarse powder and 20 g was boiled in 100 ml of double distilled water for 30 min while stirring occasionally. The aqueous extract was cooled, filtered using Whatman No.1 filter paper and stored at 4°C for further use to synthesize AgNPs from an $AgNO_3$ precursor solution.

Silver nanoparticles synthesis

Synthesis of AgNPs was carried out as described previously (Aritonang, Koleangan, and Wuntu 2019). Briefly, the aqueous extract of mangosteen peel was added to 10 ml of $AgNO_3$ solution. One milliliter of 20% plant extract was added to 50 ml of $AgNO_3$ solution, and the mixture was stirred continuously for 3 h at 90°C. In each reaction vessel, color changed to yellowish brown (Selvakumar et al. 2012). Furthermore, the mixture was stored at 4°C for the antibacterial activity test and analyzed by using UV – Vis spectrophotometer. The AgNPs were characterized by FT – IR, EDS, FESEM.

Face covering design

According to ASTM F3502–21, design criteria of face barrier coverings included setting minimum areas of face coverage over the wearer's nose and mouth. In this study, the pattern of the face covering was designed following previous research that suggested the lookalike cup mask was more suitable and comfortable for the wearer (Morishima and Mitsuno 2019). PFOA-free fluorocarbon at 2% concentration by the pad-dry-cure method was coated on the filament silk fabric (outer layer of face covering), as suggested by the minimum amount in the leaflet sheet and previous studies (Chowdhury 2018; Srichola et al. 2022). Figure 1 shows that the outermost hydrophobic layer was made of filament silk fabric (91.62 g/m^2) coated with PFOA-free fluorocarbon to improve the hydrophobic property of silk. So the water contact angle of the outermost layer was approxiamtely 133.44 ± 2.87°. The two middle filter layers comprised AgNPs coated on cotton fabric (76.61 g/m^2) and spunbond polypropylene nonwoven fabric to improve filtration efficiency of the silk face covering. The innermost layer was made of pristine eri silk fabric (74.29 g/m^2).

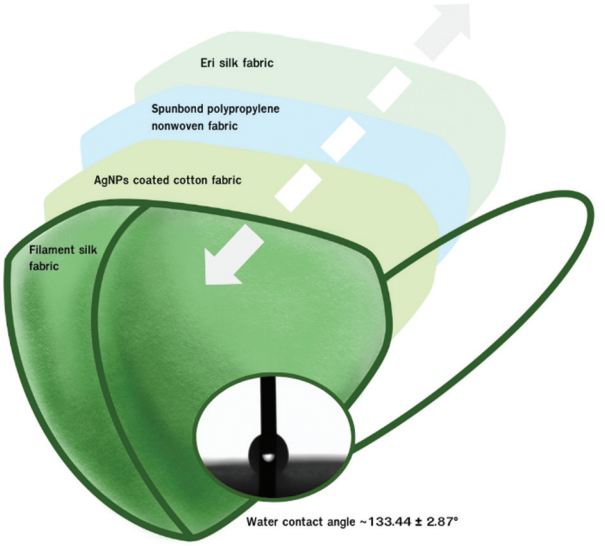

Figure 1. Design of silk face covering.

Coating of face covering with AgNPs

The outer middle layer of the face covering performed as the filtration medium and the antimicrobial layer as can be seen in Figure 1. Scoured cotton fabric (76.61 g/m^2) was coated with AgNPs by the exhausting method. An AgNPs solution (100 ppm) with 2 g/l dispersing agent was prepared following (Jha and Prasad 2016). The process was carried out at 100°C for 30 min (L:R = 1:15). Then, cotton fabric coated with AgNPs was rinsed and dried at room temperature and used to produce the outer middle layer of the silk face covering. To evaluate the durability of the AgNP-coated cotton fabric, ISO 6330:2012 was applied for 30 washing cycles.

Characterization methods

UV-visible spectroscopy

The resultant nanopowder from each of the reactions was re-suspended in an equal amount of sterile de-ionized water and spectrum cectrophotometer UV–1280 in wavelength range 200–800 nm.

Fourier transform infrared spectroscopy

Fourier transform infrared (FT–IR) spectroscopy was used to establish the identity of the phyto-chemical constituents involved in the reduction and stabilization of the silver nanoparticles. An FT–IR spectrum for powdered AgNPs was obtained using a Perkin Elmer FT–IR Spectrophotometer Frontier following the attenuated total reflectance (ATR) technique in the range 4000–500 cm^{-1}. The presence of AgNPs coated on the cotton fabric was investigated using a Thermo Scientific Nicolet IR200.

Scanning electron microscopy

Surface morphology, particle size, and composition of the AgNPs were investigated by field emission scanning electron microscopy (FESEM) using a Hitachi model, Jeol JSM-5600 LV with accelerating voltage of 2 kV and energy-dispersive X-ray spectroscopy (EDX, Zeiss Supra 35VP). Morphology, qualitative, and quantitative elemental composition of AgNPs on the cotton fabric were characterized by scanning electron microscopy (SEM), and energy-dispersive X-ray spectroscopy (EDX).

Antibacterial activity evaluation of cotton fabric

Evaluation of the antibacterial properties of the AgNP-coated cotton fabrics was conducted quantitatively according to AATCC 100–2019. *S. aureus* and *E. coli* were used as the gram positive and gram-negative organisms, respectively, according to the reference bacterial strains (Sathianarayanan et al. 2010). This test was performed on pristine cotton fabric and AgNP-coated fabric with contact time 18 h. Bacterial percentage reduction was calculated using formula (1):

$$R(\%) = \frac{B - A}{B} \times 100$$

where R = percentage reduction, A = number of bacteria recovered from inoculated treated test specimen swatches in the bottle incubated over the desired contact time and B = number of bacteria recovered from inoculated untreated test specimen swatches in the bottle incubated over the desired contact time.

Performance of the silk face covering

The performance of the developed face covering was tested according to ASTM F3502–21; sub-micron particulate filtration efficiency and airflow resistance were tested by TSI model 3082.

Results and discussion

Synthesis and characterization of the silver nanoparticles

In this study, synthesis of silver nanoparticles using *G. mangostana* peel extract as the reducing agent under optimal conditions was viewed after 3 h by color change from light yellowish to dark brown, as shown in Figure 2(a). Reduction of Ag+ to AgO in the $AgNO_3$ reaction solutions was proposed following Aminu and Oladepo (2021). Synthesis of AgNPs in the solution was also confirmed by UV–visible spectrophotometry, which exhibited the spectrum of surface plasmon resonance (SRP) with an absorption band at 420 nm (Figure 2(b)) corresponding to the classical plasmon absorption of silver metal nanoparticles in aqueous solution similar to Mowafi et al. (2017) suggested that the SRP band of silver nanoparticles in solution located between 420 and 450 nm.

EDS spectra recorded from the AgNPs are shown in Figure 3. The broad peak at 3 keV showed the presence of silver from AgNPs reduced by *G. mangostana* peel extract, concurring with Ibrahim et al. (2019). This peak showed the weight percentage of silver element at 73.37%.

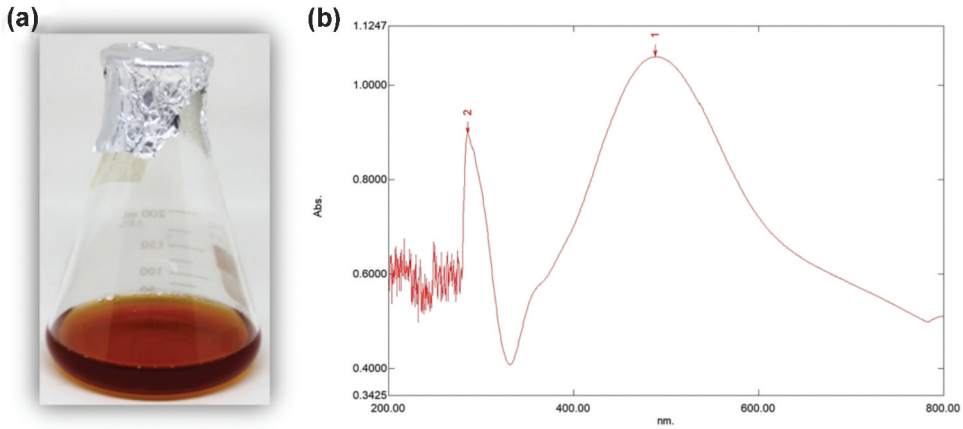

Figure 2. The synthesis of silver nanoparticles using *G. mangostana* peel extract (a) Photographs showing color changes after synthesized at 90°C for 3 h (B) UV–visible spectra of the synthesized AgNPs.

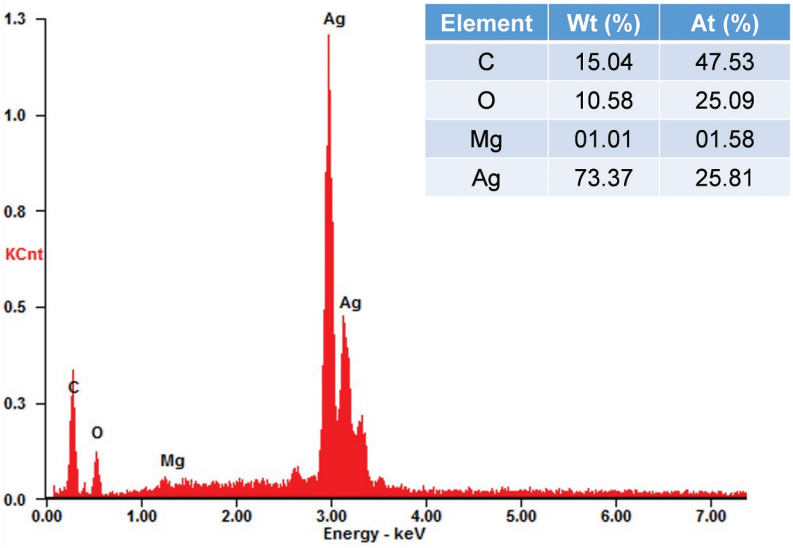

Element	Wt (%)	At (%)
C	15.04	47.53
O	10.58	25.09
Mg	01.01	01.58
Ag	73.37	25.81

Figure 3. EDS spectra recorded from a film, after formation of AgNPs different X-ray emission peaks labeled.

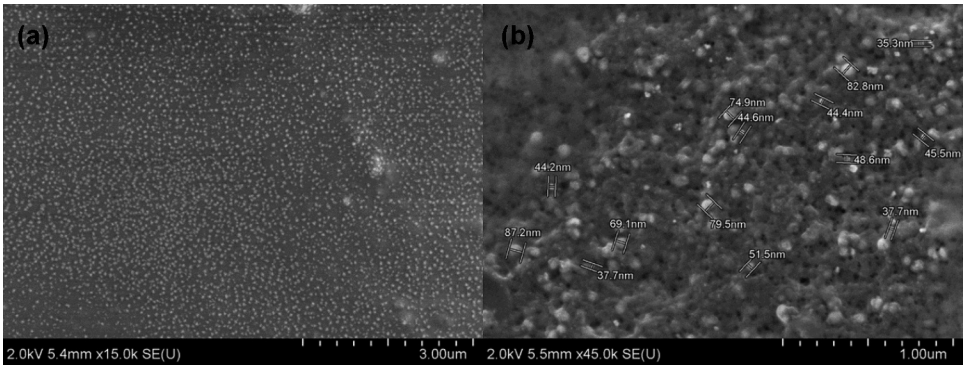

Figure 4. FESEM micrograph of AgNPs synthesized using the *G. mangostana* peel extract with accelerating voltage of 2 kV at a magnification of (A) 15000× and (B) 45000×.

The FESEM images at a magnification of 15,000 revealed small spherical grains of AgNPs (Figure 4). At a magnification of 45,000, most AgNPs in all mixtures exhibited round shapes as same as previous study (Hawar et al. 2022) with average size 40 nm (range 35–88 nm). Size particle distribution of AgNPs is shown in Figure 4, which was classified mostly (>50%) in range 21–50 micron.

Figure 5 shows the FT–IR spectra of synthesized AgNPs from *G. mangostana* peel extract after reaction with $AgNO_3$. FT–IR measurement based on AgNPs mediated by *G. mangostana* peel extract revealed different absorption peaks at 3424, 2969, 2904, 2837, 2098, 1640, 1384, 1197, 1158, 1117, 1039, 919, 827, 620, 594, 542, 416, and 408 cm^{-1}. For AgNPs, a very strong absorption peak shifted toward a lower wave number was observed at 3424 cm^{-1}, indicating binding of Ag+ with hydroxyl and or amine groups in the *G. mangostana* peel extract interacted with the surface of the AgNPs as same as the previous research (Khane et al. 2022). Other bands at 2969, 2904, and 2837 cm^{-1} were assigned to stretching vibration of the hydrocarbon (C – H) bond of alkenes, while the prominent peak at 1640 cm^{-1} indicated involvement of amide – I bond (–C=O) of proteins as a capping agent and stabilization of

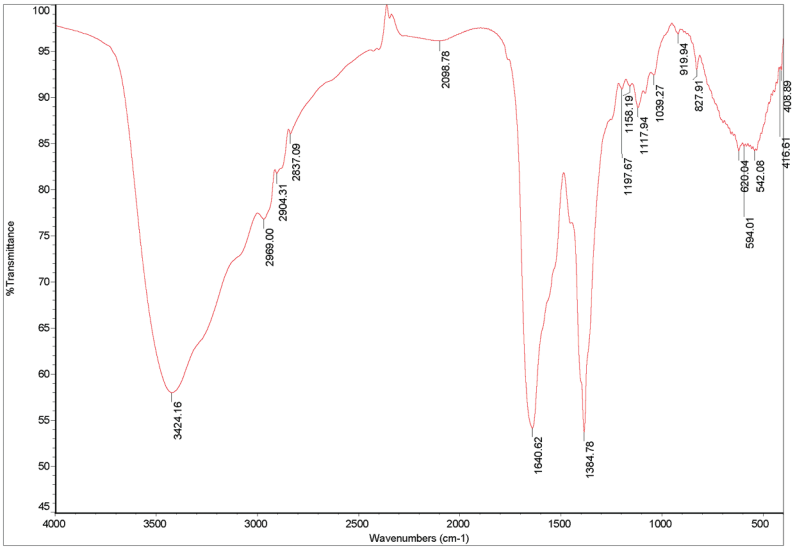

Figure 5. FT-IR spectrum of biosynthesized AgNPs by the G. mangostana peel extract.

AgNPs. The peak at 1384 cm^{-1} was assigned to C – H symmetric vibrations and also observed in *G. mangostana* peel extract (Nishanthi, Malathi, and Palani 2019).

Analysis of AgNP-coated cotton fabric

Surface morphology and the 3-dimensional nature of AgNP-coated cotton fabric (CE100) and AgNP-coated cotton fabric after 30 washing cycles (CE100-30W) were examined by SEM, with results shown in Figure 6. The SEM image of AgNP-coated cotton fabric showed clusters of silver particles concentrated in some areas of the fabric. After exposure to 30 consecutive washing cycles, the clusters of silver particles decreased and dispersed on the coated fabric surface.

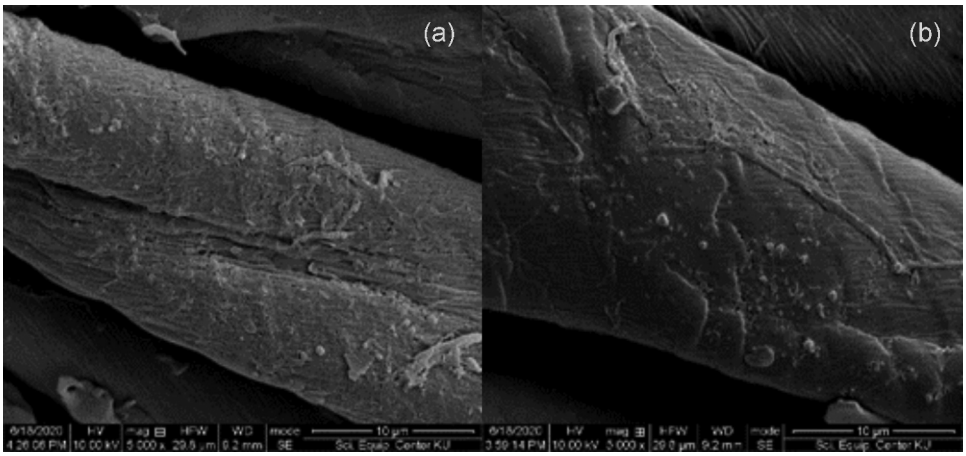

Figure 6. SEM micrograph of AgNPs coated on cotton fabric with accelerating voltage of 10 kV at a magnification of 5,000× (A) CE100 and (B) CE100-30W.

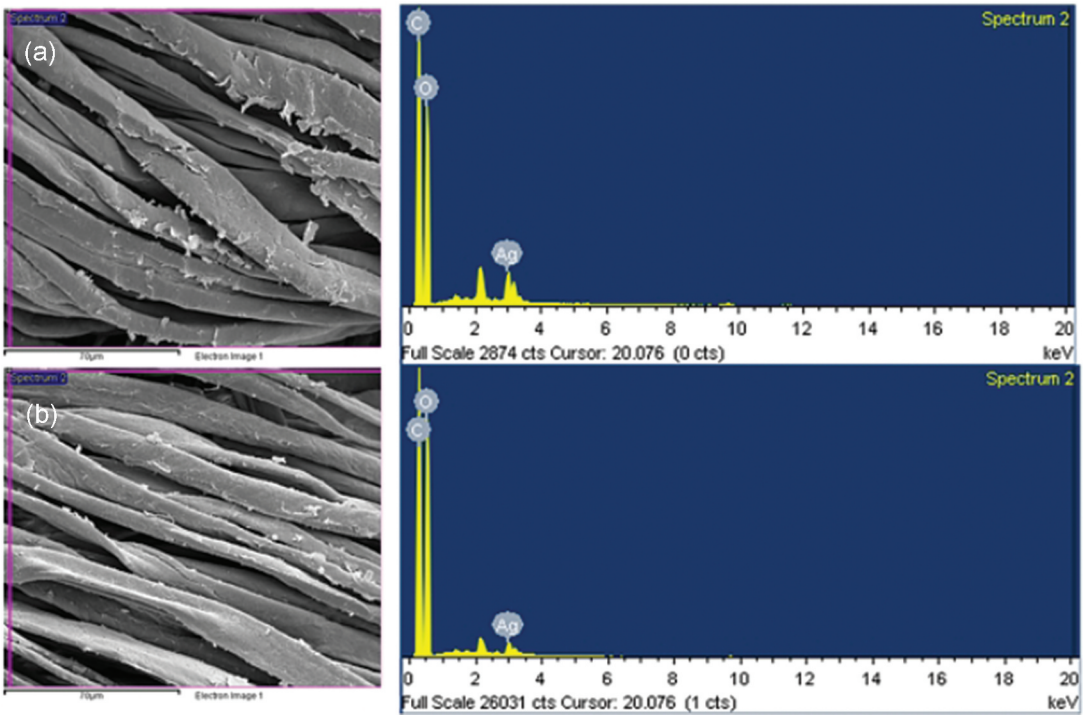

Figure 7. EDX spectroscopy of (A) CE100 and (B) CE100-30W.

Table 1. Amount of silver contained in AgNP-coated cotton fabric (CE100) and AgNP-coated cotton fabric after 30 wash cycles (CE100-30W).

Sample	Ag (% weight)
CE100	3.13 ± 0.62^{a}
CE100-30W	1.52 ± 0.10^{b}

Value are mean of triplicate measurements. Mean values with different superscript letters are significantly different ($p \leq 0.05$).

SEM equipped with EDX was employed to record the SEM images and analyzed the elemental composition of silver, as shown in Figure 7. Quantitative analysis of the silver content is shown in Table 1.

It was found the EDX spectrum of some basic elements, such as carbon and oxygen (Figure 7). The peak at 3 keV confirmed the presence of silver elements as they appeared in both AgNP-coated cotton fabric and the washed fabric samples. The elemental composition showed the presence of 3.13 and 1.52 atomic percentage of Ag at selected areas for AgNP-coated cotton fabric and AgNP-coated fabric after 30 washing cycles. This indicated that Ag content of AgNP-coated cotton fabric only slightly decreased after the washing cycles because the AgNPs were chemically bonded on the surface of the fabric (Zhang et al. 2013).

The FT – IR spectra of the uncoated cotton fabric, CE100 and CE100-30W showed different peaks as seen in Figure 8. Characteristic peaks of cotton due to cellulose macromolecules appeared at 3334 cm^{-1} (O – H stretching), 2896 cm^{-1} and 2899 cm^{-1} (C – H stretching), 1361 and 1369 cm^{-1} (C – H bending), 1029 cm^{-1} (C – O stretching) and 1000 cm^{-1} or 1012 cm^{-1} (O – H bending) (Baruah

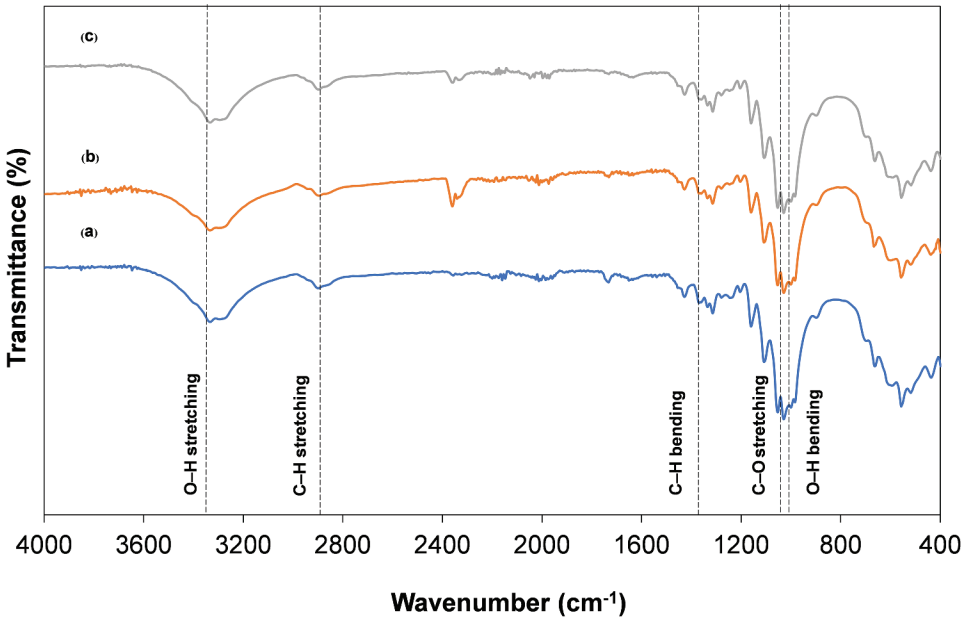

Figure 8. FT-IR spectra of (A) uncoated, (B) CE100, and (C) CE100-30W.

2016). Peaks presented at 3333–3334 cm^{-1} were assigned to O – H stretching vibration, while peaks at 2896 cm^{-1} or 2899 cm^{-1} and 1361 cm^{-1} and 1369 cm^{-1} were assigned to C – H stretching and C – H bending, respectively. The peak at 1029 cm^{-1} was related to C – O stretching, while peaks at 3334 cm^{-1} and 1012 cm^{-1} or 1018 cm^{-1} were related to O – H stretching and O – H bending, respectively. However, the FT – IR spectrum of CE100-30W was slightly different from the uncoated cotton. These results suggested that the AgNPs were chemically bonded with hydroxyl groups in cellulose macromolecules of the cotton fabric (Baruah 2016).

Antibacterial activity of AgNP-treated fabric

The uncoated cotton fabric, CE100 and CE100-30W were challenged with *E. coli* and *S. aureus*. Viable bacterial counts recovered from the fabrics before and after incubation are shown in Table 2. After 18 h of incubation, the AgNP-coated fabric showed percentage reduction in viable *E. coli* and *S. aureus* at 99.92% and 99.94%, respectively. After 30 washing cycles, the antibacterial activity did not significantly decrease, with percentage reductions in viable *E. coli* and *S. aureus* 99.96% and 99.96%. So the washing process was slightly affected to the antimicrobial properties similar to some previous studies (Aladpoosh, Montazer, and Samadi 2014; Maghsoudi et al. 2022; Xu et al. 2017). This indicated that the AgNPs were

Table 2. Viable bacterial counts (cfu/ml) at zero and 18-h contact time intervals with uncoated cotton fabric (CE), CE100, and CE100-30W.

	E. coli			*S. aureus*		
	Number of microorganisms (cfu/ml)		% Reduction	Number of microorganisms (cfu/ml)		% Reduction
Sample	0	18		0	18	
CE	1.23×10^5	1.800×10^8	0.00^a	1.70×10^5	1.86×10^7	0.00^a
CE100	1.23×10^5	<100	99.92^b	1.70×10^5	<100	99.94^b
CE100-30W	2.40×10^5	<100	99.96^b	2.30×10^5	<100	99.96^b

Value are mean of triplicate measurements. Mean values with different superscript letters are significantly different ($p \leq 0.05$).

Table 3. Performance properties of the barrier face covering.

ASTM F3502–21 (Level II)	Criterion	Result
Sub-micron particulate filtration efficiency at 0.1 micron (%)	≥50	67.98
Airflow resistance, inhalation (mm H_2O)	<5.0	2.87

Value are mean of triplicate measurements.

fixed on the cotton fabric surface because of electrostatic attractions between oppositely charged AgNPs and the surface of the cotton fiber (Zhang et al. 2013). It could be referred that this face covering mask was durability enough as it could be used more than 30 times with the retained antibacterial activity. A clinical test in mice at a dose of 2000 mg/kg AgNPs resulted in no death or injury (Kim et al. 2013). Thus, this green technique of AgNP biosynthesis can be applied as a cotton fabric filter in the outer middle layer of the face covering to add antibacterial property.

Sub-micron particle filtration efficiency and airflow resistance

The principal performance properties of the developed silk barrier face covering are shown in Table 3. Sub-micron particulate filtration efficiency was 67.98%, which met the requirement of Level II of ASTM F3502 standard but was not comparable to the N95 respirator, which was at least 95% (Forouzandeh, O'Dowd, and Pillai 2021). This silk barrier was effective for public use during the COVID-19 pandemic. However, Skaria and Smaldone (2014) found that the airflow pressure of the three-layer surgical mask and N95 respirator was about 1.87 and 2.67 mm H_2O respectively. So this developed face covering might be less comfort to wear than the three-layer surgical mask and N95 respirator according to this face covering compiled with four layers. However, the developed silk face covering was comfortable enough for breathing and suitable to wear on a daily basis.

Conclusions

The outer middle layer of the silk face covering consisting of biosynthetic AgNPs coated on cotton fabric enhanced antimicrobial properties and filtration efficiency. Silver nanoparticle-coated cotton fabrics showed good particle dispersion, while percentage reduction of *E. coli* and *S. aureus* did not change after 30 washing cycles. Silk face coverings with AgNP-coated cotton fabric as the outer middle layer, filament silk fabric as the outermost layer and eri silk fabric as the innermost layer offered acceptable sub-micron particle filtration efficiency and airflow resistance at 67.98% and 2.87 mm H_2O, respectively. These values met the requirement of ASTM classification for barrier face coverings at level II performance. Further studies should focus on the durability of this silk face covering as an important property of textile goods.

Highlights

- Biosynthesized silver nanoparticles from mangosteen peel extract were spherical with particle sizes ranging from 35 to 88 nm.
- A solution of 100 ppm silver nanoparticles was successfully coated on cotton fabric by the exhaustion method, with clusters of silver particles concentrated in some areas. Antibacterial properties did not significantly change after 30 washing cycles.
- This silk face covering with an antibacterial layer of silver nanoparticle coated cotton fabric had 0.1 micron particle size filtration efficiency of 67.98% and airflow resistance 2.87 mm H_2O, which met the requirement of level II ASTM performance classification.

Acknowledgements

This research study was financially supported by Kasetsart University Research and Development Institute (KURDI). The authors are also grateful to the Department of Medical Sciences, Ministry of Public Health and the Microbiological Resources Centre, Thailand Institute of Scientific and Technological Research (TISTR) for microorganism support.

Disclosure statement

No potential conflict of interest was reported by the authors.

Funding

This work was supported by Kasetsart University Research and Development Institute (KURDI)

ORCID

Phannaphat Phromphen http://orcid.org/0000-0001-8989-9419
Udomlak Sukatta http://orcid.org/0000-0002-5666-7838
Prapassorn Rugthaworn http://orcid.org/0000-0002-2229-1465
Jirachaya Boonyarit http://orcid.org/0000-0002-5481-5155
Phitalai Phoophat http://orcid.org/0000-0003-1580-4231
Nattadon Rungruangkitkrai http://orcid.org/0000-0001-6273-6177
Pawarin Tuntariyanond http://orcid.org/0000-0003-0203-7766
Nawarat Chartvivatpornchai http://orcid.org/0000-0002-4418-6199
Thanyachol Apipatpapha http://orcid.org/0000-0002-4396-7794
Rungsima Chollakup http://orcid.org/0000-0002-9659-7854

References

Abou Elmaaty, T. M., H. Elsisi, G. Elsayad, H. Elhadad, and M. R. Plutino. 2022. Recent advances in functionalization of cotton fabrics with nanotechnology. *Polymers* 14:4273. doi:10.3390/polym14204273.

Adanur, S., and A. Jayswal. 2020. Filtration mechanisms and manufacturing methods of face masks: An overview. *Journal of Industrial Textiles* 51:3683S–717S. doi:10.1177/1528083720980169.

Aladpoosh, R., M. Montazer, and N. Samadi. 2014. In situ green synthesis of silver nanoparticles on cotton fabric using Seidlitzia rosmarinus ashes. *Cellulose* 21:3755–66. doi:10.1007/s10570-014-0369-1.

American Society for Testing and Materials. 2021. *ASTM F3502-21 Standard specification for barrier face coverings*.

Aminu, A., and S. A. Oladepo. 2021. Fast orange peel-mediated synthesis of silver nanoparticles and use as visual colorimetric sensor in the selective detection of mercury (II) ions. *Arabian Journal for Science & Engineering* 46:5477–87. doi:10.1007/s13369-020-05030-3.

Aritonang, H. F., H. Koleangan, and A. D. Wuntu. 2019. Synthesis of silver nanoparticles using aqueous extract of medicinal plants' (*Impatiens balsamina* and *Lantana camara*) fresh leaves and analysis of antimicrobial activity. *International Journal of Microbiology* 2019:1–8. doi:10.1155/2019/8642303.

Bankar, A., B. Joshi, A. R. Kumar, and S. Zinjarde. 2010. Banana peel extract mediated novel route for the synthesis of silver nanoparticles. *Colloids and Surfaces A, Physicochemical and Engineering Aspects* 368:58–63. doi:10.1016/j.colsurfa.2010.07.024.

Baruah, B. 2016. In situ and facile synthesis of silver nanoparticles on baby wipes and their applications in catalysis and SERS. *RSC Advances* 6:5016–23. doi:10.1039/c5ra20059h.

Brahmachari, G., S. Sarkar, R. Ghosh, S. Barman, N. C. Mandal, S. K. Jash, B. Banerjee, and R. Roy. 2014. Sunlight-induced rapid and efficient biogenic synthesis of silver nanoparticles using aqueous leaf extract of *Ocimum sanctum* Linn. with enhanced antibacterial activity. *Organic and Medicinal Chemistry Letters* 4:1–10. doi:10.1186/s13588-014-0018-6.

Chollakup, R., and W. Smitthipong. 2012. Evolution of mulberry and non-mulberry silk fibers for textile applications. In *Silk: Properties, production and uses*, ed. A. Pornanong, 41–86. New York: Nova Science Publishers, Inc.

Chowdhury, K. P. 2018. Process intensification of fluorocarbon – free and fluorocarbon-based water repellent finishes on cotton knit fabrics. *Journal of Textile Engineering & Fashion Technology* 4:232–40. doi:10.15406/jteft.2018.04.00146.

Davies, A., K. A. Thompson, K. Giri, G. Kafatos, J. Walker, and A. Bennett. 2013. Testing the efficacy of homemade masks: Would they protect in an influenza pandemic? *Disaster Medicine and Public Health Preparedness* 7:413–18. doi:10.1017/dmp.2013.43.

Emam, H. E., M. H. El-Rafie, H. B. Ahmed, and M. K. Zahran. 2015. Room temperature synthesis of metallic nanosilver using acacia to impart durable biocidal effect on cotton fabrics. *Fibers and Polymer* 16:1676–87. doi:10.1007/s12221-015-5197-x.

Emam, H. E., M. H. El-Rafie, and M. Rehan. 2021. Functionalization of unbleached flax fibers by direct integration of nano-silver through internal and external reduction. *Fibers Polymer* 22:3014–24. doi:10.1007/s12221-021-0993-y.

Emam, H. E., and M. K. Zahran. 2015. Ag(^{0}) nanoparticles containing cotton fabric: Synthesis, characterization, color data and antibacterial action. *International Journal of Biological Macromolecules* 75:106–14. doi:10.1016/j.ijbiomac.2014.12.050.

Forouzandeh, P., K. O'Dowd, and S. C. Pillai. 2021. Face masks and respirators in the fight against the COVID–19 pandemic: An overview of the standards and testing methods. *Safety Science* 133:104995. doi:10.1016/j.ssci.2020.104995.

Hao, W., A. Parasch, S. Williams, J. Li, H. Ma, J. Burken, and Y. Wang. 2020. Filtration performances of non-medical materials as candidates for manufacturing facemasks and respirators. *International Journal of Hygiene & Environmental Health* 229. doi:10.1016/j.ijheh.2020.113582.

Hasan, K. M. F., H. Wang, S. Mahmud, A. Islam, M. A. Habib, and C. Genyang. 2022. Enhancing mechanical and antibacterial performances of organic cotton materials with greenly synthesized colored silver nanoparticles. *International Journal of Clothing Science and Technology* 34:549–65. doi:10.1108/IJCST-05-2021-0071.

Hawar, S. N., H. S. Al-Shmgani, Z. A. Al-Kubaisi, G. M. Sulaiman, Y. H. Dewir, J. J. Rikisahedew, and A. Omri. 2022. Green synthesis of silver nanoparticles from *Alhagi graecorum* leaf extract and evaluation of their cytotoxicity and antifungal activity. *Journal of Nanomaterials* 2022:1–8. doi:10.1155/2022/1058119.

Hiragond, C. B., A. S. Kshirsagar, V. V. Dhapte, T. Khanna, P. Joshi, and P. V. More. 2018. Enhanced anti-microbial response of commercial face mask using colloidal silver nanoparticles. *Vacuum* 156:475–82. doi:10.1016/j.vacuum.2018.08.007.

Ibrahim, H. 2015. Green synthesis and characterization of silver nanoparticles using banana peel extract and their antimicrobial activity against representative microorganisms. *Journal of Radiation Research & Applied Sciences* 8:265–75. doi:10.1016/j.jrras.2015.01.007.

Ibrahim, E., H. Fouad, M. Zhang, Y. Zhang, W. Qiu, C. Yan, B. Li, J. Mo, and J. Chen. 2019. Biosynthesis of silver nanoparticles using endophytic bacteria and their role in inhibition of rice pathogenic bacteria and plant growth promotion. *RSC Advances* 9:29293–99. doi:10.1039/C9RA04246F.

Jha, K., and A. K. Prasad. 2016. Green synthesis and antimicrobial activity of silver nanoparticles onto cotton fabric: An amenable option for textile industries. *Advanced Materials Letters* 7:42–46. doi:10.5185/amlett.2016.6083.

Kaur, J., R. Rajkhowa, T. Afrin, T. Tsuzuki, and X. Wang. 2014. Facts and myths of antibacterial properties of silk. *Biopolymers* 101:237–45. doi:10.1002/bip.22323.

Khane, Y., K. Benouis, S. Albukhaty, G. M. Sulaiman, M. M. Abomughaid, A. Al Ali, D. Aouf, F. Fenniche, S. Khane, W. Chaibi, et al. 2022. Green synthesis of silver nanoparticles using aqueous Citrus limon zest extract: Characterization and evaluation of their antioxidant and antimicrobial properties. *Nanomaterials* 12:2013. doi:10.3390/nano12122013.

Kharaghani, D., M. Q. Khan, A. Shahzad, Y. Inoue, T. Yamamoto, S. Rozet, Y. Tamada, and I. S. Kim. 2018. Preparation and in-vitro assessment of hierarchal organized antibacterial breath mask based on polyacrylonitrile/silver (PAN/AgNPs) nanofiber. *Nanomaterials* 8:461. doi:10.3390/nano8070461.

Kim, J. S., K. S. Song, J. H. Sung, H. R. Ryu, B. G. Choi, H. S. Cho, J. K. Lee, and I. J. Yu. 2013. Genotoxicity, acute oral and dermal toxicity, eye and dermal irritation and corrosion and skin sensitisation evaluation of silver nanoparticles. *Nanotoxicology* 7:953–60. doi:10.3109/17435390.2012.676099.

Konda, A., A. Prakash, G. A. Moss, M. Schmoldt, G. D. Grant, and S. Guha. 2020. Aerosol filtration efficiency of common fabrics used in respiratory cloth masks. *ACS Nano* 14:6339–47. doi:10.1021/acsnano.0c03252.

Kora, A., and R. Sashidhar. 2015. Antibacterial activity of biogenic silver nanoparticles synthesized with gum ghatti and gum olibanum: A comparative study. *The Journal of Antibiotics* 68:88–97. doi:10.1038/ja.2014.114.

Li, Y., P. Leung, L. Yao, Q. W. Song, and E. Newton. 2006. Antimicrobial effect of surgical masks coated with nanoparticles. *The Journal of Hospital Infection* 62:58–63. doi:10.1016/j.jhin.2005.04.015.

Lima, L. N., D. C. Reis, V. K. Sakano, M. A. Franco, F. G. Morais, and V. M. John. 2022. Influence of microstructure and physical characteristics in the performance of non-professional masks sold in São Paulo. *Public Health* 205:90–98. doi:10.1016/j.puhe.2022.01.009.

MacIntyre, C. R., H. Seale, T. C. Dung, N. T. Hien, P. T. Nga, A. A. Chughtai, B. Rahman, D. E. Dwyer, and Q. Wang. 2015. A cluster randomised trial of cloth masks compared with medical masks in healthcare workers. *British Medical Journal Open* 5:e006577. doi:10.1136/bmjopen-2014-006577.

Maghsoudi, S., P. N. Pour, H. Ebrahimnejad, E. Jalali, and M. Zangiabadi. 2022. Decoration of cotton fiber with biosynthesized Ag/Zno nanocomposite for durable antibacterial textile. *Journal of Natural Fibers* 19:8033–43. doi:10.1080/15440478.2021.1958433.

Mohammed, A. M., K. T. Hassan, and O. M. Hassan. 2023. Assessment of antimicrobial activity of chitosan/silver nanoparticles hydrogel and cryogel microspheres. *International Journal of Biological Macromolecules* 233:123580. Advance online publication. doi:10.1016/j.ijbiomac.2023.123580.

Morishima, M., and T. Mitsuno. 2019. Analysis of hygienic face mask patterns for young people. *Textile Research Journal* 89:4670–80. doi:10.1177/0040517519840635.

Mowafi, S., M. Rehan, H. M. Mashaly, A. Abou El-Kheir, and H. E. Emam. 2017. Influence of silver nanoparticles on the fabrics functions prepared by *in-situ* technique. *The Journal of the Textile Institute* 108:1828–39. doi:10.1080/00405000.2017.1292649.

Nakkala, J. R., R. Mata, E. Bhagat, and S. R. Sadras. 2015. Green synthesis of silver and gold nanoparticles from *Gymnema sylvestre* leaf extract: Study of antioxidant and anticancer activities. *Journal of Nanoparticle Research* 17:1–15. doi:10.1007/s11051-015-2957-x.

Nishanthi, R., S. Malathi, and P. Palani. 2019. Green synthesis and characterization of bioinspired silver, gold and platinum nanoparticles and evaluation of their synergistic antibacterial activity after combining with different classes of antibiotics. *Materials Science & Engineering C* 96:693–707. doi:10.1016/j.msec.2018.11.050.

Parlin, A. F., S. M. Stratton, T. M. Culley, P. A. Guerra, and N. J. Hickok. 2020. A laboratory-based study examining the properties of silk fabric to evaluate its potential as a protective barrier for personal protective equipment and as a functional material for face coverings during the COVID-19 pandemic. *PLos One* 15:e0239531. doi:10.1371/journal.pone.0239531.

Phoophat, P., P. Kumphai, S. Suwonsichon, J. Boonyarit, C. Plangmon, and R. Chollakup. 2020. Application of Kawabata evaluation system for the tactile properties of woven silk fabrics in textile industry. *IOP Conference Series: Materials Science and Engineering* doi: 10.1088/1757-899X/773/1/012035.

Ray, S. S., Y. I. Park, H. Park, S. E. Nam, I. C. Kim, and Y. N. Kwon. 2020. Surface innovation to enhance anti-droplet and hydrophobic behavior of breathable compressed-polyurethane masks. *Environmental Technology & Innovation* 20:101093. doi:10.1016/j.eti.2020.101093.

Rungruangkitkrai, N., R. Mongkholrattanasit, P. Phoophat, N. Chartvivatpornchai, S. Sirimungkararat, K. Wongkasem, P. Tuntariyanond, N. Nithithongsakol, and R. Chollakup. 2020. UV-protection property of Eri silk fabric dyed with natural dyes for eco-friendly textiles. *IOP Conference Series: Materials Science and Engineering* doi: 10.1088/1757-899X/773/1/012027.

Sathianarayanan, M. P., N. V. Bhat, S. S. Kokate, and V. E. Walunj. 2010. Antibacterial finish for cotton fabric from herbal products. *Indian Journal of Fibre & Textile Research* 35:50–58.

Selvakumar, P., S. Viveka, S. Prakash, S. Jasminebeaula, and R. Uloganathan. 2012. Antimicrobial activity of extracellularly synthesized silver nanoparticles from marine derived *Streptomyces rochei*. *Journal of Pharmaceutical and Biological Sciences* 3:188–97. doi:10.1016/j.ejar.2016.05.004.

Skaria, S. D., and G. C. Smaldone. 2014. Respiratory source control using surgical masks with nanofiber media. *The Annals of Occupational Hygiene* 58:771–81. doi:10.1093/annhyg/meu023.

Srichola, P., J. Boonyarit, W. Kongtud, and R. Chollakup. 2022. Utilization of pineapple leaf fiber mixed with banana or cattail stem fibers and their paper physical properties for application in packaging. *Agricultural Natural Resources* 56:1103–12. doi:10.34044/j.anres.2022.56.6.05.

Syafiuddin, A. 2019. Toward a comprehensive understanding of textiles functionalized with silver nanoparticles. *Journal of the Chinese Chemical Society* 66:793–814. doi:10.1002/jccs.201800474.

World Health Organization. 2020. Mask use in the context of COVID–19. Last Modified December 1, 2020. Accessed August 1, 2022. https://www.who.int/publications/i/item/advice-on-the-use-of-masks-in-the-community-during-home-care-and-in-healthcare-settings-in-the-context-of-the-novel-coronavirus-(2019-ncov)-outbreak

Xu, Q., J. Gu, Y. Zhao, X. Ke, and X. Liu. 2017. Antibacterial cotton fabric with enhanced durability prepared using L-cysteine and silver nanoparticles. *Fibers and Polymers* 18:2204–11. doi:10.1007/s12221-017-7567-z.

Yaqoob, A. A., K. Umar, and M. N. M. Ibrahim. 2020. Silver nanoparticles: Various methods of synthesis, size affecting factors and their potential applications–a review. *Applied Nanoscience* 10:1369–78. doi:10.1007/s13204-020-01318-w.

Zhang, D., L. Chen, C. Zang, Y. Chen, and H. Lin. 2013. Antibacterial cotton fabric grafted with silver nanoparticles and its excellent laundering durability. *Carbohydrate Polymers* 92:2088–94. doi:10.1016/j.carbpol.2012.11.100.

Zhao, M., L. Liao, W. Xiao, X. Yu, H. Wang, Q. Wang, Y. L. Lin, F. S. Kilinc-Balci, A. Price, L. Chu, et al. 2020. Household materials selection for homemade cloth face coverings and their filtration efficiency enhancement with triboelectric charging. *Nano Letters* 20:5544–52. doi:10.1021/acs.nanolett.0c02211.

Zhao, Z. Y., P. J. Li, R. S. Xie, X. Y. Cao, D. L. Su, and Y. Shan. 2022. Biosynthesis of silver nanoparticle composites based on hesperidin and pectin and their synergistic antibacterial mechanism. *International Journal of Biological Macromolecules* 214:220–29. doi:10.1016/j.ijbiomac.2022.06.048.